

Vehicle Three-Dimensional Pose and Shape Estimation from Multiple Monocular Vision

Wenhai Ding¹, Shuaijun Li², Guilin Zhang², Xiangyu Lei², Huihuan Qian² and Yangsheng Xu²

Abstract—This paper proposes an accurate approach to estimate vehicles’ 3D pose and shape from multi-view monocular images with a small overlap. This approach utilizes a state-of-the-art convolutional neural network (CNN) to detect vehicles’ semantic keypoints in images and then introduces a Cross Projection Optimization (CPO) method to estimate the 3D pose accurately. During the iterative CPO process, it implements a new vehicle shape adjustment method named Hierarchical Wireframe Constraint (HWC). The approach is tested under both simulated and real-world scenes for performance verification. It’s shown that this approach outperforms other existing monocular and stereo visual methods for vehicles’ 3D pose and shape estimation. This approach provides new and robust solutions for accurate visual vehicle localization, and it can be applied to the massive surveillance camera networks for intelligent transportation applications such as automatic driving assistance.

I. INTRODUCTION

Most recently, road scene understanding is well studied for improving the perception ability of automatic driving. Meanwhile, 3D pose estimation for objects becomes a hot research topic, owing to its significance to the field of robotics. These factors motive us to focus on pose and shape estimation of vehicles.

To estimate vehicle’s pose information, despite sensors such as LiDAR, depth camera and stereo camera have been used, their application scopes are constrained due to their high cost and limited usage in real world. Therefore, more and more works concentrate on monocular visual estimation methods, which can be potentially applied to the massive prevailing surveillance cameras in the real world to make a huge impact.

In fact, mobile robots are always conducted using on-board visions, which is called simultaneous localization and mapping (SLAM) [8], [9], [10]. In contrast, off-board vision can also be considered for 3D pose estimation tasks. Considering that off-board vision usually has the advantage of possessing a better field-of-view (FOV), and that many of the latest deep-learning based computer vision technics are developed based on external vision, there is a huge potential

This research is supported by the NSFC project U1613226 from the State Joint Engineering Lab and Shenzhen Engineering Lab on Robotics and Intelligent Manufacturing, China.

¹Wenhai Ding is with the Department of Electronic Engineering, Tsinghua University, Haidian District, Beijing, China dwh14@mails.tsinghua.edu.cn

²Shuaijun Li, Guilin Zhang, Xiangyu Lei, Huihuan Qian and Yangsheng Xu are with the Robotics and Artificial Intelligence Laboratory, The Chinese University of Hong Kong, Shenzhen, Shenzhen, China sjli01@mae.cuhk.edu.hk, {gl.zhang.cuhk, x.y.lei.hk}@gmail.com, {hhqian, ysxu}@mae.cuhk.edu.hk

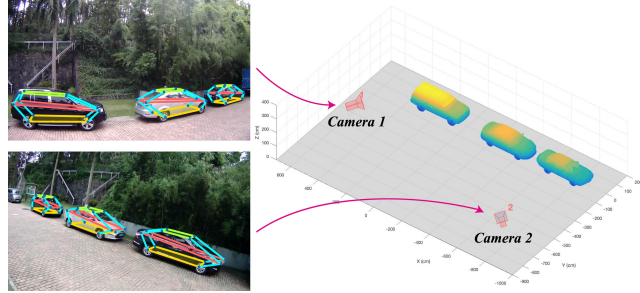


Fig. 1. Example of pose and shape estimation. Left two images come from two different view cameras, respectively. Wireframes projected on the images represent estimation results. On the right side, three vehicles are placed in a 3D space according to the estimated pose and CAD models.

to use off-board visions for vehicle 3D pose estimation tasks.

In recent works on vision-based 3D pose estimation, deep learning tools of CNN are used. Keypoints of a series of objects are defined and detected to aid with the pose estimation [22]. Those CNN methods provide a new way to solve this kind of problem. But in most cases, a single image is processed for estimating task and this suffers from several drawbacks. For one thing, the robustness of the keypoint detection is poor when vehicle occultation (by trees, walls, or other vehicles, etc.) are considered. For another, according to the principle of 3D projection, depth of object depends entirely on the scale of the model. The translation error increases when the model used is inaccurate even if an accurate pose is provided. These drawbacks can be greatly improved if multiple images from different views can be used together for 3D pose and shape estimation.

Based on the background above, we propose an approach using multiple off-board cameras (two at least) with a small overlap to obtain 3D pose and shape of vehicles. An example result of our approach is shown in Fig. 1. Compared with methods with bounding box annotation [4], our proposed approach utilizes a wireframe model to describe vehicle’s 3D pose and shape information accurately.

The whole processing pipeline is divided into two stages as shown in Fig. 2. First, in CNN stage, multiple images are taken from cameras of different views (two images are used mostly for discussion simplification), and then they are fed into a coarse-to-fine hourglass CNN [1], which is specially trained for vehicle semantic keypoints detection. After CNN processing, two sets of keypoints are obtained as an output. Second, in optimization stage, the information from these two sets of keypoints are combined using our CPO method. This method projects a general 3D vehicle model onto each

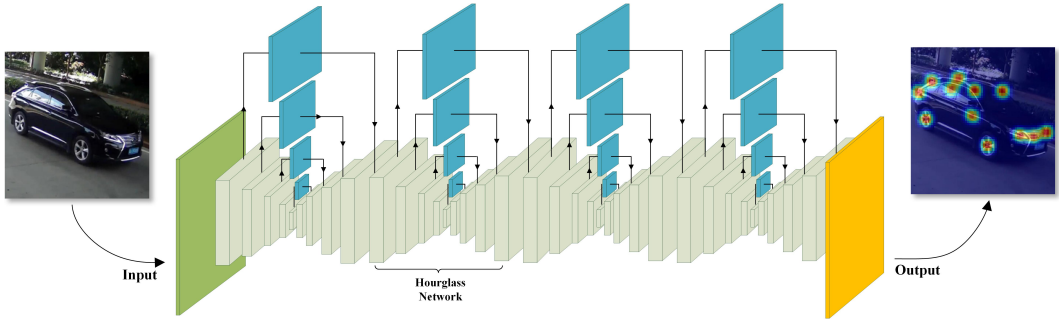


Fig. 2. **Overview of our approach.** Stage 1 consists the steps of CNN process which outputs heatmaps with highlight keypoint positions. Stage 2 utilizes results of the previous stage as input and start to fuse the information from multiple images. Our core algorithm comes next, with the methods of pose estimation (CPO) and shape adjustment (HWC), an accurate pose and shape estimation is obtained. Here, a CAD vehicle model is used for better display.

image and conducts a pose estimation process by iteratively minimizing the projection errors. It's worth mentioning that no prior knowledge about target vehicle is required in this approach. Vehicle's shape estimation is realized by a shape adjustment process which uses a general 3D vehicle model as a starting point, and implements HWC method during the CPO iterations.

A series of tests have been conducted to evaluate the performance of our proposed approach, using both vehicle images from a robot simulation software environment, and vehicle images taken from the real world. The evaluation results show that our proposed approach estimates vehicle's 3D pose and shape information accurately and robustly, achieving less than 3° of rotation error and 5 cm of translation error. In pace with traffic surveillance's popularity in cities and rural areas, it is practical for those overlapping cameras to form a navigation system to satisfy automatic driving localization requirements, guide automatic parking system for collision avoidance, and realize other localization applications.

II. RELATED WORKS

A. Convolutional Neural Network

The past few decades have witnessed the development of neural networks, especially in the field of complex feature detection. [2], [3] are state-of-the-art works of object detection. Ren *et al.* [2] provided a real-time region proposal network to detect multiple objects on the 2D image. Joseph *et al.* [3] proposed a detection method which can achieve the classification of 9,000 objects. All these detection methods help localization algorithm to focus mainly on their target.

For most detection and estimation tasks, ConvNet is used to recognize complex and high-level features, which cannot be sufficiently tackled by traditional computer vision methods. Lately, there are already some end-to-end methods for pose estimation. [13], [11] presented data-driven methods for 3D object reconstruction from a single image. [12], [4] utilized video or multi-channel information obtained from on-board device to localize vehicles.

In the recent study, a stacked hourglass framework [1] was proposed to detect semantic keypoints on the bodies of human beings. Owing to its coarse-to-fine architecture,

features can be detected on multiple resolutions, leading to high accuracy results. Our approach follows this direction and takes advantages of this architecture. We train our CNN on a vehicle dataset which is part of PASCAL3D+ [30]. Compared to traditional random forests means like [16], this method can output keypoints' position more accurately.

B. 3D Vehicle Localization

In the field of robotics and computer vision, vehicle localization is always at the cutting edge [23], [24]. Both on-board and off-board methods have representative works.

On-board methods are always trying to solve the problem called SLAM. Some significant works can obtain an accurate pose in large scale with a monocular camera [8], a stereo camera [9] or a depth camera [10]. Other sensors like GPS, Encoder and IMU are also introduced as on-board device for localization task [21]. Although SLAM has become the mainstream method of localization, off-board methods are also considered to have great potential.

Most of the off-board works combine a single image with complex vehicle models. Zhu *et al.* [31] used constrained discriminative parts and predefined wireframe models to estimate the 3D pose. [19] proposed a similarity measure method with off-board camera, and a top-down perception approach is proposed in [32]. Works mentioned above all require a complex accurate car model, besides their feature detecting methods are not robust for arbitrary scene and viewpoint. To simplify the estimation pipeline, some end-to-end methods are proposed. [13] and [11] directly trained a CNN with a single image and 3D landmarks, but complex and large annotation dataset limits the usage this method.

The latest works [6], [7] combined semantic keypoints with simple models. Using accurate CNN method provides them with large advantages in pose estimation. These approaches outperformed most existing estimation methods. However, methods with single image have a problem between translation error and model scale. Even if [6] and [7] have shape adjustment in their process, inaccurate model results in errors.

C. Multi-camera System

Most of multi-camera systems are applied to the field of human pose estimation, such as [14], [15] and [16]. Pavlakos

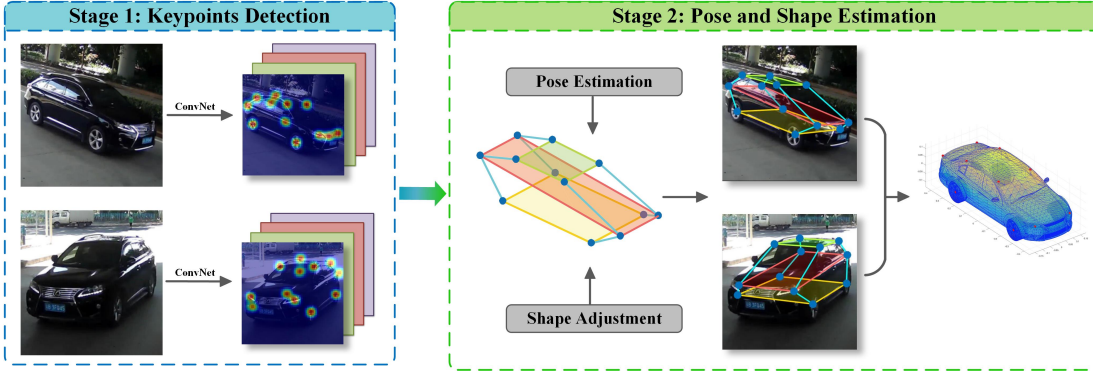


Fig. 3. **CNN with Stacked hourglass architecture.** Four-layer hourglass architecture is used in our algorithm. The original image is put into the left side while the output heatmaps are obtained from the right side. Each sub-network has a intermediate output, which can be used for intermedia supervision. The basic module in each hourglass is called residual module, which can extract high-level features and remain original feature at the same time.

et al. [16] utilized random forest to classify each pixel in each image, [14] recovered a volumetric prediction from multiple images. The standard principle of human pose estimation is using 3D pictorial structure, which has been proved to be effective. Our method is inspired by these approaches to combine image features with a deformable model.

In consideration of vehicle localization, there are few works using multiple cameras or stereo cameras. Chen *et al.* [4] used bird view lidar data and front image to localize surrounding vehicles for the purpose of automatic driving, but only rough 3D bounding box results are given in this approach. [17] and [18] improved SLAM algorithm by integrating multi-view cameras and shape information. They outperformed some traditional SLAM methods. Calibrated stereo camera with small baseline can be used to reconstruct depth of the scene like [20] and [5], but the narrow overlapping region is not wide enough for accurate vehicle localization. Although some defects still exist, works mentioned above prove the superiority of multi-view approaches and guide us to explore more possibilities in this direction.



Fig. 4. **Examples of our CNN output.** Different views are chosen to show the robustness of this CNN framework, and all these images come from a multi-view dataset [28]. As results show, blocked annotations can still be localized with relatively high confidence.

D. Our Contribution

Considering all the pros and cons of existing single-image and multi-image methods, we introduce a new framework for vehicle 3D localization. First, multiple cameras are led into to solve the problem of model scale. Second, 2D keypoints detection datasets are easier to get than 3D landmarks. Third, wireframe model provides more accurate description of vehicles. Our contributions are as follows:

- We propose an accurate pose estimating approach with small-overlap multi-view cameras. This approach utilizes CPO method to combine keypoint detecting information from different views.
- We introduce a specially designed shape adjustment method (HWC) to restrict the vehicle model during the estimation process. This method helps us to describe the shape of vehicle's main frame more concretely.
- We evaluate our approach on both simulated and real-world scene. Empirically, our method outperforms existing monocular and multi-view methods in respects of pose estimation and shape similarity error.

III. TECHNICAL METHOD

The pipeline of our approach consists of two stages, keypoints detection and pose estimation. The process of pose estimation includes shape adjustment, which can improve the accuracy of estimation result.

A. Semantic Keypoints Detection

Before keypoints detection, the range of interest (ROI) is required for selecting vehicles from images with 2D bounding box. As 2D object detection has been well studied for a period of time, we assume that ROIs have been provided by state-of-the-art methods [3] mentioned in Section II.

Leveraging the recent success in keypoints detection like [23], [25], we use a four-layer hourglass stacked network introduced by [1]. The framework is shown in Fig. 3. This network framework has a symmetric architecture with residual module as its basic unit. This module contains both original information and high-level feature. A single hourglass network consists several residual modules, which

can achieve top-down and bottom-up process. During one hourglass process, keypoint features can be extracted from both global and local resolutions. Another novel method used in this network is intermediate supervision. For every hourglass architecture, intermediate stage outputs a heatmap result, which can help solve the vanishing gradient problem.

This neural network has gained great success in human body semantic keypoints localization and it demonstrates that stacked architecture outperforms monolithic top-down networks [26], [27]. As for our task, this framework is trained on about 4,000 images from vehicle annotation part of PASCAL3D+ as well as our own dataset. We find that a four-layer framework works well for our task. Some qualitative detection result samples are shown in Fig. 4.

During the training stage, we input a label with 12 annotations (wheel \times 4, light \times 4, windshield \times 2, rear window \times 2). A noteworthy thing is that self-concealed keypoints are also annotated, so the CNN will learn the whole structure of vehicles at the same time. Therefore, outputs of our network are always 12 heatmaps, each of which has a 2D Gaussian distribution. The value of the Gaussian distribution denotes the probability of the keypoint position. Generally, obscured parts are always inaccurate in output heatmaps, and different views affect the CNN output as well. Then, in some cases, a single image may reason about wrong pose estimation with some keypoints that seriously deviate from real values. Considering this phenomenon, multi-view images are combined to avoid overly relying on one inaccurate image.

B. Pose and Shape Estimation

To accurately estimate 3D pose and shape of vehicles, we propose an approach named CPO. This approach projects general 3D model to each image, and minimizes the projection error globally to get an accurate pose and shape. During the iterative process, the shape of the vehicle is adjusted under some constraints in HWC. And for the sake of simplicity, we only consider the situation of two cameras.

Initial Weight Matrix: As we have semantic keypoints location from CNN for two images, we can integrate the information that which view has the best confidence for each keypoints. As two sets of heatmaps come from the same network, subtracting the two CNN outputs gives us the information about occultation and wrong detection. Then, a normalized weight can be obtained:

$$\begin{aligned}\psi_{i,j}^k &= \mu_1 w_{i,cnn}^k + \mu_2 (w_{i,cnn}^k - w_{j,cnn}^k) \\ w_{i,nor}^k &= \frac{\psi_{i,j}^k}{\sum_{k=1}^K \psi_{i,j}^k}\end{aligned}\quad (1)$$

The superscript i, j means camera 1 and 2. Then a diagonal weight matrix can be represented as

$$W = \begin{bmatrix} w_{i,nor}^{i,1} & \dots & 0 \\ \vdots & \ddots & \vdots \\ 0 & \dots & w_{i,nor}^{i,K} \end{bmatrix}\quad (2)$$

Elements in this weight matrix are on behalf of the importance of each keypoint during the estimation process.

Single Camera Iteration: For each camera, we can estimate 3D pose from single image with a general model as approaches presented by [6] and [7]. Here we use singular value decomposition (SVD) method [29] for rigid motion estimation.

Denote the initial pose of our model by P , and the number of keypoints is K , then we can represent each 3D annotation as p_i where $i \in [1, K]$. The minimal projection error pose is denoted by Q , then we seek a rotation R and a translation vector t such that

$$(R, t) = \underset{R \in SO(d), t \in \mathbb{R}^d}{\operatorname{argmin}} \sum_{i=1}^n w_i \| (Rp_i + t) - q_i \|^2, \quad (3)$$

where w_i means the weight getting from (2). Within several iterations, the model can be transformed close to the position where minimal projection error is obtained.

Multi-view Information Combination: In one iteration, we do least-squares process for both cameras separately. After that, we minimize an energy function defined for cross projections:

$$f(t) = \frac{1}{2} \sum_{i=1}^c \left(\sum_{j=1}^c W(t)_i \|\mathcal{L}_{i,j}(t)\|_F^2 \right) \quad (4)$$

where t denotes the iteration time and $\mathcal{L}_{i,j}$ means the projection error from model optimized by camera i to image plane j . Meanwhile, the weight matrix is updated along with iteration, and the criterion is defined for combining multi-view information:

$$\begin{aligned}w_i^k(t+1) &= \mu_1 w_i^k(t) + \mu_2 \|\mathcal{L}_{i,j}(t)\|_F^2 \\ &\quad + \mu_3 (w_{i,nor}^k(t) - w_{j,nor}^k(t))\end{aligned}\quad (5)$$

Here, the first term on the right-hand side means the weight value for keypoint k in last iteration, and the second term represents the projection error from camera i to image j . The last item evaluates the visibility between two cameras. Updating weight matrix can help reaching a global maximum point for both cameras smoothly, as well as dynamically adjusting the importance of each keypoint.

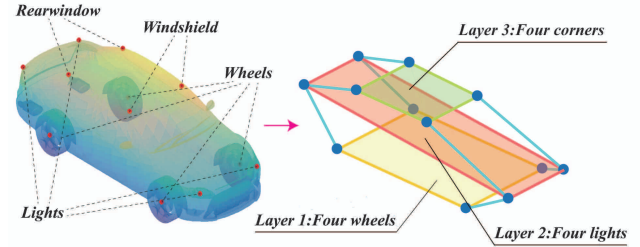


Fig. 5. **Explanation of HWC method.** A mean vehicle shape is acquired from several CAD models as the left image shows and four kinds of annotations are signed with notes. From this abstract model, a three-layer wireframe is introduced and constrained by some principles.

Hierarchical Wireframe Constraint: With a view to vehicles, they all have a common general framework, in which every part has certain location. Moreover, inside the

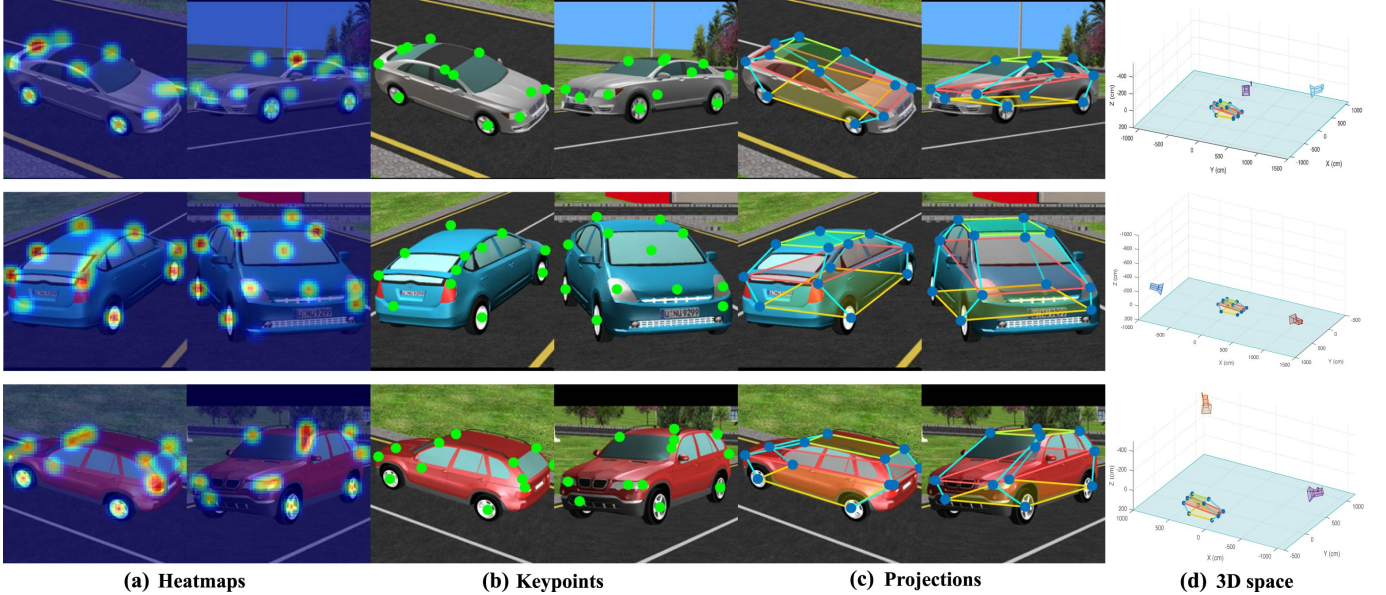


Fig. 6. Qualitative results showing pose and shape estimation of webots simulation platform. Every row displays a vehicle class and a different view combination. (a) shows the CNN outputs of two different views. (b) shows the keypoints of maximum probability in two cameras' heatmaps. (c) shows projection of estimated pose and shape on both camera images. (d) shows a 3D space where real vehicle wireframe models are placed in.

vehicle class, some degrees of freedom are available, such as the distance between light and wheel and the angle between wheel-plane and light-plane. Considering all the fixed and flexible rules, we design a constraint method for hierarchical models. Models under this principle are divided into three layers, as shown in Fig. 5. These three layers are formed by 4 rooftop points, 4 light points and 4 wheel points, and each layer represents a plane. Since vehicles are highly symmetrical, we can define some general criterions during shape adjustment:

- Each layer should be vertical and symmetrical to the medial surface.
- Wheel layer should be a standard rectangle, while other two layers can be extended into a trapezoidal in a certain range.
- The relationship between layers has a high degree of freedom for different kinds of vehicles.
- Distance between two points is flexible but within certain maximum.

Shape Adjustment: With the HWC method mentioned above, we can gradually correct the wireframe model during the pose estimating process. The method like [7] separated pose estimation and shape adjustment into two stages, but it is very possible that inaccurate shape leads pose estimation into local minimum points.

When doing shape adjustment, we optimize each point with (4) using constrained optimization algorithm for multivariate functions. Four points which are in the same layer are considered together. For each layer, HWC method is applied. In order to keep a symmetric architecture, a weighted average method is introduced:

$$p^k(x, y) = w_{i,project}^k p_i^k(x, y) + w_{j,project}^k p_j^k(x, y) \quad (6)$$

$$\text{s.t. } w_{i,project}^k + w_{j,project}^k = 1$$

where k means the number of keypoints, and two normalized weight coefficients come from projection error and keypoint weight value. $p^k(x, y)$ denotes the new 3D position of keypoint k . Across layers, maximal moving step size is set in case of resulting in a large deformation. Doing shape adjustment with totally wrong pose is risky, so some pure pose estimation iterations are processed firstly until a relatively smooth energy function value is obtained.

After reaching the maximum iteration or minimum threshold between two adjacent iterations, the whole process stops. In most instances, optimized results from two cameras are almost the same, but when there is a deviation between them, we choose the smaller projection error one as our final result.

IV. EXPERIMENTS

This section verifies the performance of our algorithm under both simulated and real-world conditions.

Webots is a development environment used to model, program and simulate mobile robots. By building up simulation environment and importing experimental vehicle models from the database, our algorithms can be quickly and effectively verified. Besides, accurate ground truths of models can be accessed easily according to the coordinate system inside the software. The extrinsic and intrinsic parameters of cameras used in the experiments can also be calibrated of convenience with a fake chessboard. Vast amounts of data are collected for preliminary works of this paper by conducting experiments under simulation environment.

Moreover, real-world experiments are also conducted to verify the practicality and robustness of our algorithm. Test results of a series of experiments using real vehicles are covered in this section.

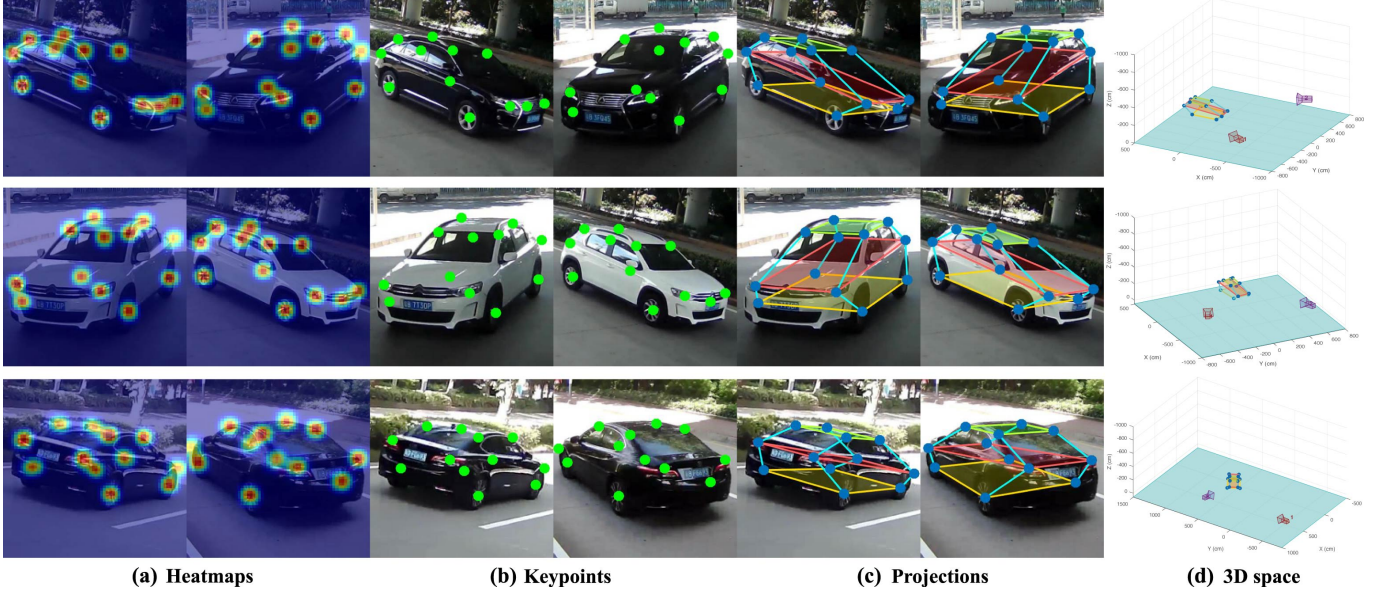


Fig. 7. Qualitative results showing pose and shape estimation of real cars. Every row displays a vehicle class and a different view combination. (a) shows the CNN outputs of two different views. (b) shows the keypoints of maximum probability in two cameras' heatmaps. (c) shows projection of estimated pose and shape on both camera images. (d) shows a 3D space where real vehicle wireframe models are placed in.

TABLE I
KEYPOINT DISTANCE ERROR (CM)

Approach	Left Front Wheel	Right Front Wheel	Left Back Wheel	Right Back Wheel	Left Front Light	Right Front Light	Left Back Light	Right Back Light	Left-up Winds- shield	Right-up Winds- shield	Left-up Rear Window	Right-up Rear Window	Mean
6DOF-LINCON	18.73	14.50	28.29	30.73	12.33	8.99	27.97	32.39	15.84	12.95	58.60	55.71	26.42
6DOF-TOYOTA	37.21	42.33	70.02	66.87	27.14	29.91	75.74	75.01	50.17	53.13	87.28	82.33	58.10
6DOF-BWM	29.65	28.60	40.09	39.39	23.98	25.80	45.84	40.84	15.44	10.95	25.75	23.05	29.12
6DOF-MEAN	28.53	28.48	46.14	45.66	21.15	21.57	49.85	49.41	27.15	25.68	57.21	53.70	37.88
OURS-LINCON	7.30	7.39	6.59	5.12	6.03	5.90	13.32	12.56	7.17	6.98	25.48	24.58	10.78
OURS-TOYOTA	8.48	10.21	10.52	8.11	7.30	7.17	14.20	14.20	7.99	7.86	32.87	33.33	13.52
OURS-BWM	3.15	2.94	3.79	4.60	4.96	4.93	8.99	9.96	5.96	4.73	17.41	14.03	7.12
OURS-MEAN	6.31	6.85	6.97	5.94	6.10	6.00	12.17	12.24	7.04	6.52	25.25	23.98	10.48
Harvesting	N/A	N/A	N/A	N/A	N/A	N/A	N/A	N/A	N/A	N/A	N/A	N/A	5.689

A. Simulated experiments using Webots

We use Webots as our simulation platform to collect data for CNN and our proposed algorithm. Three kinds of vehicle models were imported from the database, including Lincoln MKZ, Toyota Prius and BMW X5, and a live-similar environment was built up. For each vehicle model, we have tested about 50 image groups, and in each group, there are two images with known camera parameters. Vehicles and other objects of the environment in Webots are observed in the view of perspective projection, which ensures that the photos taken in this platform are perspective projected. Then, a chessboard with size of $2m \times 3m$ was chosen to calibrate the extrinsic and intrinsic parameters of individual monocular cameras (less than 0.2 pixels error). Ground truths represented by 3D coordinates of the 12 semantic keypoints were recorded.

Photos taken from different views were then used to predict the semantic keypoints of vehicles using the pre-trained CNN. Heatmaps were produced to record the gaussian distribution of the predicted semantic keypoints. Parts of the test results are shown in Fig. 6. To evaluate our approach, we consider errors of this experiment in two different metrics. First, the errors of the 12 semantic keypoints of vehicles with respect to those of the ground truths of the vehicle models can be expressed as euclidean distance. Second, the errors of orientation and translation of the estimated pose with respect to the ground truths can be expressed as below:

$$\Delta(R_1, R_2) = \frac{\|\log(R_1^T R_2)\|_F}{\sqrt{2}} \quad (7)$$

$$\Delta(T_1, T_2) = \left\| \frac{\sum_{k=1}^K p_1^k}{K} - \frac{\sum_{k=1}^K p_2^k}{K} \right\| \quad (8)$$

where the rotation error is represented as geodesic distance and the translation error is represented as distance between the centroids of two point sets.

Keypoints localization errors in 3D space are shown in Table I, including the comparison with a state-of-the-art method [6]. We notice that although sometimes outputs of the CNN are not accurate, final keypoints position is extremely close to the ground truth in our approach, due to the HWC shape adjustment method. The algorithm of [6] uses only single image, so we recorded the best result of two images. After testing algorithms on three different kinds of vehicle (each has more than 100 images), we reach the conclusion that less keypoint distance error is achieved compared with single image approach [6]. It is worth discussing that rear window and tail lamp points are more inaccurate than others. One reason to explain this phenomenon is that those keypoints change relatively large inside vehicle classes, resulting in inaccurate output of CNN keypoints detector. Despite with these detection errors, rotation and translation error can still be controlled below a low level.

As contrast, a result of human pose estimation from multi-view images is given in the last row of Table I. But volume of human body is smaller than vehicle's. Taking into account the proportion of errors to the whole object, we can still achieve a better result.

TABLE II
POSE ESTIMATION ERROR

Approach	Rotation (degree)			Translation (cm)
PNP	7.17		46.6452	
6DOF-WEAK [6]	7.99		N/A	
6DOF-FULL [6]	5.57		27.5758	
Viewpoint [23]	9.10		N/A	
Reconstruct [7]	8.79	12.57	16.16	N/A
ObjProp3D [5]	17.37	21.86	26.87	N/A
3DVP [13]	11.1873			N/A
OURS-webots	4.4134			6.2150
OURS-realcar	2.8757			4.7365

B. Real World

This section verifies the performances of our algorithm under real-world conditions. The pipeline of conducting real-world experiments is similar to that of the simulation experiments. A series of vehicles representing different car models were selected to be processed by the proposed algorithm. Ground truths were recorded, and the camera parameters were calibrated with a chess board in advance. The real-world estimation results are shown in Fig. 7.

Similarly, we consider errors of the estimated poses and translation with (8) and (9). Results are recorded in Table II, including comparisons with other estimation algorithms. What needs to be explained is that translation error cannot be obtained for some monocular methods. For [7] and

ObjProp3D [5], those three results are obtained on three different difficulty level datasets of KITTI [33].

At last, we discuss the defect of single-image method in detail. When the recovered 3D models of vehicles generated by the single monocular image algorithm is projected to the imaging plane of another camera, the estimated pose is usually observed to be inaccurate. The explanation for the occurrence of these results is that the scale of the deformable model is not determined accurately with selected vehicle models, and then, the depth from the recovered model to the imaging plane is not accurately determined. The situation is shown in Fig. 8, where the original model is smaller than real size.

V. CONCLUSIONS

In this paper, we present an accurate approach to estimate pose and shape of vehicles with multiple cameras. We propose a cross projection optimization scheme and a deformable model constrain method to make the best of the information from multiple images. We evaluate our method on both simulated platform and real world, and demonstrate superior performance than published monolithic and stereo algorithms. We achieved less than 3° and 5 cm error in aspect of rotation and translation.

Even with imprecise keypoint localization, our method still presents robustness, which is significant in robotics and auto-driving. Moreover, precise 3D dimensions, owing to the accurate wireframe description of the shape, can improve the ability of collision avoidance and motion planning.

In terms of application prospects of our approach, modern surveillance camera networks have enough resolution for object detection and pose estimation. Additionally, surveillance cameras usually have common visual field which gives our algorithm an opportunity to be applied. Based on these hardware systems, more accurate vehicle localization can be achieved with the help of our algorithm.

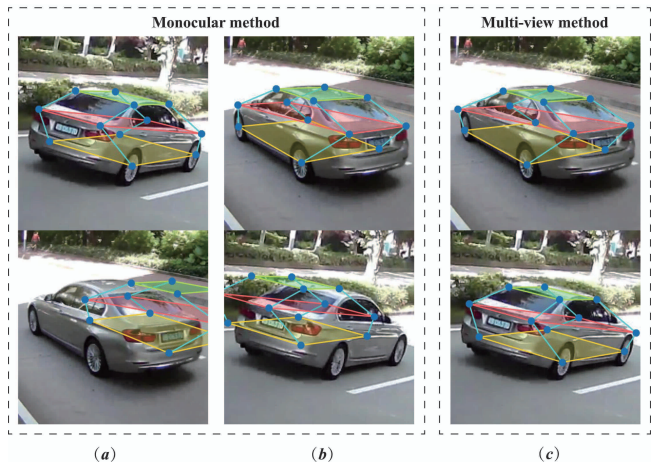


Fig. 8. **Comparison between monocular method and multi-view method.** (a) shows the result that only relies on camera 1, and the bottom image is the projection to another camera's image plane. (b) is the same with (a), except for relying on camera 2. (c) are projection results achieved by CPO and HWC method.

REFERENCES

[1] A. Newell, K. Yang and J. Deng, "Stacked Hourglass Networks for Human Pose Estimation," in *Proc. 2016 European Conf. on Comput. Vision (ECCV)*, Amsterdam, Netherlands, 2016, pp. 483-499.

[2] S. Ren, K. He, R. Girshick and J. Sun, "Faster R-CNN: Towards Real-Time Object Detection with Region Proposal Networks," *IEEE Trans. on Pattern Anal. and Mach. Intell. (TPAMI)*, vol. 39, no. 6, pp. 1137-1149, 2017.

[3] J. Redmon, S. Divvala, R. Girshick and A. Farhadi, "YOLO 9000: Better, Faster, Stronger," in *Proc. 2017 IEEE Conf. on Comput. Vision and Pattern Recognition (CVPR)*, Hawaii, USA, 2017.

[4] X. Chen, H. Ma, J. Wan, B. Li and T. Xia, "Multi-View 3D Object Detection Network for Autonomous Driving," in *Proc. 2017 IEEE Conf. on Comput. Vision and Pattern Recognition (CVPR)*, Hawaii, USA, 2017.

[5] X. Chen, K. Kundu, Y. Zhu, A. G. Berneshawi, H. Ma, S. Fidler and R. Urtasun, "3D Object Proposals for Accurate Object Class Detection", in *Proc. 2015 Advances in Neural Inform. Process. Syst. (NIPS)*, Montreal, Canada, 2015.

[6] G. Pavlakos, X. Zhou, A. Chan, K. G. Derpanis and K. Daniilidis, "6-DoF Object Pose from Semantic Keypoints," in *Proc. 2017 IEEE Int. Conf. on Robotics and Automation (ICRA)*, Singapore, Singapore, 2017.

[7] J. K. Murthy, G V. S. Krishna, F. Chhaya and K. M. Krishna, "Reconstructing Vehicles from a Single Image: Shape Priors for Road Scene Understanding," in *Proc. 2017 IEEE Int. Conf. on Robotics and Automation (ICRA)*, Singapore, Singapore, 2017, pp. 724-731.

[8] J. Engel, T. Schöps and D. Cremers, "LSD-SLAM: Large-Scale Direct Monocular SLAM," in *Proc. 2014 European Conf. on Comput. Vision (ECCV)*, Zurich, Swiss, 2014, pp. 834-849.

[9] R. Mur-Artal and J. D. Tardós, "ORB-SLAM2: An Open-Source SLAM System for Monocular, Stereo, and RGB-D Cameras," *IEEE Trans. on Robotics*, early access, 2017.

[10] T. Qin, P. Li and S. Shen, "VINS-Mono: A Robust and Versatile Monocular Visual-Inertial State Estimator," *arXiv preprint arXiv:1708.03852*, 2017.

[11] C. Häne, S. Tulsiani and J. Malik, "Hierarchical Surface Prediction for 3D Object Reconstruction," *arXiv preprint arXiv:1704.00710*, 2017.

[12] T. Zhou, M. Brown, N. Snavely and D. G. Lowe, "Unsupervised Learning of Depth and Ego-Motion from Video," *arXiv preprint arXiv:1704.07813*, 2017.

[13] Y. Xiang, W. Choi, Y. Lin, and S. Savarese, "Data-Driven 3D Voxel Patterns for Object Category Recognition, Silvio Savarese," in *Proc. 2015 IEEE Conf. on Comput. Vision and Pattern Recognition (CVPR)*, Boston, USA, 2015, pp. 1903-1911.

[14] G. Pavlakos, X. Zhou, K. G. Derpanis and K. Daniilidis, "Harvesting Multiple Views for Marker-less 3D Human Pose Annotations," in *Proc. 2017 IEEE Conf. on Comput. Vision and Pattern Recognition (CVPR)*, Hawaii, USA, 2017.

[15] V. Belagiannis, S. Amin, M. Andriluka, B. Schiele, N. Navab and S. Ilic, "3D pictorial structures revisited: Multiple human pose estimation," *IEEE Trans. on Pattern Anal. and Mach. Intell.*, vol. 38, no. 10, pp. 1929-1942, 2016.

[16] V. Kazemi, M. Burenius, H. Azizpour and J. Sullivan, "Multiview body part recognition with random forests," in *Proc. 24th British Mach. Vision Conf. (BMVC)*, Bristol, UK, 2013.

[17] F. Chhaya, D. Reddy, S. Upadhyay, V. Chari, M. Z. Zia and K. M. Krishna, "Monocular Reconstruction of Vehicles: Combining SLAM with Shape Priors," in *Proc. 2016 IEEE Int. Conf. on Robotics and Automation (ICRA)*, Stockholm, Sweden, 2016, pp. 5758-5765.

[18] A. Das and S. L. Waslander, "Calibration of a Dynamic Camera Cluster for Multi-Camera Visual SLAM," in *Proc. 2016 IEEE Int. Conf. on Intell. Robots and Syst. (IROS)*, Daejeon, Korea, 2016, pp. 4637-4642.

[19] S. Hoermann, P. V. K. Borges, "Vehicle Localization and Classification Using Off-Board Vision and 3-D Models," *IEEE Trans. on Robotics*, vol. 30, no. 2, pp. 432-447.

[20] B. Barrois, S. Hristova, C. Wohler, F. Kummertand, and C. Hermes, "3D Pose Estimation of Vehicles Using a Stereo Camera," in *Proc. 2009 IEEE Intell. Vehicles Symp. (IV)*, Xi'an, China, 2009, pp. 267-272.

[21] J. K. Suhr, J. Jang, D. Min and H. G. Jung, "Sensor Fusion-Based Low-Cost Vehicle Localization System for Complex Urban Environments," *IEEE Trans. on Intell. Transportation Systems*, vol. 18, no. 5, pp. 1078-1086.

[22] M. Z. Zia, M. Stark and K. Schindler, "Towards Scene Understanding with Detailed 3D Object Representations," *Int. J. of Comput. Vision*, vol. 112, no. 2, pp. 188-203, 2015.

[23] S. Tulsiani and J. Malik, "Viewpoints and Keypoints," in *Proc. 2015 IEEE Conf. on Comput. Vision and Pattern Recognition (CVPR)*, Boston, USA, 2015, pp. 1510-1519.

[24] S. Azam, A. Rafique and M. Jeon, "Vehicle Pose Detection Using Region Based Convolutional Neural Network," in *Proc. 4th Int. Conf. on Control, Automation and Inform. Sci. (ICCAIS)*, Taiyuan, China, 2016, pp. 194-198.

[25] Y. Sun, X. Wang and X. Tang, "Deep Convolutional Network Cascade for Facial Point Detection," in *Proc. 2013 IEEE Conf. on Comput. Vision and Pattern Recognition (CVPR)*, Portland, USA, 2013, pp. 3476-3483.

[26] J. J. Tompson, A. Jain, Y. LeCun and C. Bregler, "Joint training of a convolutional network and a graphical model for human pose estimation," in *Proc. 2014 Advances in Neural Inform. Process. Syst. (NIPS)*, Montreal, Canada, 2014.

[27] S. Wei, V. Ramakrishna, T. Kanade and Y. Sheikh, "Convolutional Pose Machines," in *Proc. 2016 IEEE Conf. on Comput. Vision and Pattern Recognition (CVPR)*, Las Vegas, USA, 2016, pp. 4724-4732.

[28] M. Ozuysal, V. Lepetit and P. Fua, "Pose Estimation for Category Specific Multiview Object Localization," in *Proc. 2009 IEEE Conf. on Comput. Vision and Pattern Recognition (CVPR)*, Miami, USA, 2009, pp. 778-785.

[29] O. Sorkine-Hornung and M. Rabinovich, "Least-squares rigid motion using SVD," *Tech. Rep.*, vol. 120, no. 3, pp. 52, Department of Computer Science, ETH, Zurich, 2009.

[30] Y. Xiang, M. Roozbeh and S. Silvio, "Beyond PASCAL: A Benchmark for 3D Object Detection in the Wild," in *Proc. 2014 IEEE Winter Conf. on Applications of Comput. Vision (WACV)*, Steamboat Springs, USA, 2014, pp. 75-82.

[31] M. Zhu, X. Zhou and K. Daniilidis, "Pose and Shape Estimation with Discriminatively Learned Parts," *Comput. Sci.*, vol. 29, no. 6, no. 419-424, 2015.

[32] C. Bernay-Angeletti, F. Chabot, C. Aynaud, R. Aufre and R. Chauvin, "A Top-down Perception Approach for Vehicle Pose Estimation," in *2015 IEEE Int. Conf. on Robotics and Biomimetics (ROBIO)*, Zhuhai, China, 2015, pp. 2240-2245.

[33] A. Geiger, P. Lenz and R. Urtasun, "Are we ready for Autonomous Driving? The KITTI Vision Benchmark Suite," in *Proc. 2012 IEEE Conf. on Comput. Vision and Pattern Recognition (CVPR)*, Rhode Island, USA, 2012, pp. 3354-3361.